Biomechanical Characterization of the Temporomandibular Joint Disc

Fazaeli, S.

2019

document version
Publisher's PDF, also known as Version of record

CHAPTER 3

Alteration of Structural and Mechanical Properties of the Temporomandibular Joint Disc Following Elastase Digestion

Sepanta Fazaeli, Fereshteh Mirahmadi,
Vincent Everts, Theodoor Henri Smit,
Jan Harm Koolstra, Samaneh Ghazanfari

Manuscript under review

Abstract

The temporomandibular joint disc is a fibrocartilaginous structure, composed of collagen fibers, elastin fibers and proteoglycans. Despite the crucial role of elastin fibers in load-bearing properties of connective tissues, its contribution in temporomandibular joint disc biomechanics has been disregarded. This study attempts to characterize the structural-functional contribution of elastin in the temporomandibular joint disc. Using elastase, we selectively perturbed the elastin fiber network in porcine temporomandibular joint discs and investigated the structural, compositional and mechanical regional changes through: (1) analysis of collagen and elastin fibers by immunolabeling and transmission electron microscopy; (2) quantitative analysis of collagen tortuosity, cell shape and disc volume; (3) biochemical quantification of collagen, glycosaminoglycan and elastin content; and (4) cyclic compression test. Following elastase treatment, microscopic examination revealed fragmentation of elastin fibers across the temporomandibular joint disc, with a more pronounced effect in the intermediate regions. Also, the biochemical analyses of the intermediate regions showed significant depletion of elastin, and substantial decrease in collagen and glycosaminoglycan content, likely due to non-specific activity of elastase. Degradation of elastin fibers affected the homeostatic configuration of the disc, reflected in its significant volume enlargement accompanied by remarkable reduction of collagen tortuosity, and cell elongation. Mechanically, intermediate regions in the treated samples exhibited a significant increase in their maximal energy dissipation while their instantaneous modulus was not significantly affected. We conclude that elastin fibers contribute to the restoration and maintenance of the disc resting shape and actively interact with collagen fibers to provide mechanical resilience to the temporomandibular joint disc.

Key words: Temporomandibular joint disc; Cartilage; Elastin fiber; Mechanical properties; Enzymatic degradation.

1. Introduction

The temporomandibular joint (TMJ) disc is a highly deformable and yet robust fibrocartilaginous tissue that overlies the articulating surfaces of the mandibular condyle and temporal fossa providing smooth jaw movement. The disc plays a crucial role as a shock absorber, force distributor and a congruent agent of the articulating structures in complex jaw kinematics [1, 2]. Morphologically, it has a saddle-shaped structure being thicker at the posterior and anterior edges and thinner in the intermediate regions.
The extracellular matrix (ECM) of the disc is mainly composed of a highly organized and dense collagenous network, encompassing interstitial fluid, elastin fibers and a minimal amount of proteoglycans and glycosaminoglycans (GAGs) [3-5]. The region-dependent distribution, organization and interaction of these elements yield to a heterogeneous and anisotropic mechanical behavior of the disc under various loading conditions during jaw movement [6, 7].

The structural-functional characteristics of the TMJ disc may be compromised under pathological conditions. One of the most ambiguous areas of clinical dentistry is temporomandibular disorder (TMD). Approximately, 10% of the population exhibit symptoms of TMD [8], among which 70% demonstrate malpositioning of the disc, known as internal derangement [9]. Although the etiology of disc pathology remains unknown, it has been suggested that the internal derangement may alter the ECM composition of the disc, subjecting it to abnormal loading conditions, which could lead to its degeneration and subsequent deterioration [10, 11]. This standpoint is of high importance considering the presence of degradative enzymes as well as their endogenous inhibitors in the ECM. Disturbing their delicate balance by any intrinsic or extrinsic factor may result in a surplus of enzymatic activity in the matrix, altering ECM composition and structure and eventually leading to mechanical failure of the tissue [12-15]. Structural-functional characterization of the individual structural elements of the TMJ disc can help to achieve a better understanding of the pathophysiology of the TMJ disc derangement; to establish design criteria for construction of a biocompatible tissue-engineered replica; and to develop more accurate computational prediction models.

Elastin fibers of different tissues have been characterized extensively in recent studies [16-22]. In these studies, selective enzymatic degradation techniques were used in combination with mechanical testing, biochemical analysis or microscopic examination to assess the contribution of elastin fibers in connective tissue biomechanics. In response to loading, connective tissues exhibit heterogeneous, anisotropic and hyperelastic behavior where expansion of the tissue (i.e. proteoglycan-driven swelling pressure in cartilage) is restricted by collagen [23, 24] and to a lesser extent by elastin fibers [25]. Collagen fibers are responsible for providing stiffness and strength to the tissue at higher strains while elastin fibers, co-distributed within a collagenous network, are believed to act as springs, accounting for elasticity of the ECM [25, 26]. More specifically, elastin fibers store elastic energy, thereby preserving collagen for damage through impact loading [16, 17, 22, 27] and contributing to recovery of the tissue after straining [17, 26, 28, 29]. This is particularly relevant for compliant structures like the TMJ disc.

While the mechanical contribution of collagen fibers has been extensively studied, there are only few studies on the occurrence and distribution of elastin fibers in the TMJ disc [4, 29-40]. Therefore, the aim of the present study is to provide a systematic structural-functional characterization of elastin fibers in the TMJ disc, in light of their contribution in healthy and degenerated conditions. We used selective enzymatic degradation of elastin fibers in combination with microscopic, biochemical and mechanical analyses to elucidate the nature and extent of elastin fiber contribution to TMJ disc biomechanics. We investigated five different regions known to possess a different quantity and organization of ECM constituents [41]: posterior band (PB), anterior band (AB), intermediate zone central (IZC), intermediate zone medial (IZM) and intermediate zone lateral (IZL).

2. Materials and methods

2. 1. Sample preparation

A total of ten young porcine heads were obtained from a local abattoir immediately after slaughter. The TMJ discs with intact condylar heads were harvested *en bloc.* The discs were then removed from extraneous parts and discarded when any gross abnormality was observed. Next, the discs were washed in phosphate buffered saline (PBS), and wrapped in gauze soaked in a solution of PBS and protease inhibitors (Roche Diagnostics, Germany). Prior to their use, the discs were stored at -20 °C.

2. 2. Enzymatic digestion

Given the sample variations regarding their thickness, biochemical composition and mechanical properties, our main goal was to find a sufficient combination of enzyme concentration and incubation time resulting in a partial degradation of elastin fibers, so that the samples maintain sufficient integrity to undergo post treatment mechanical test. We based our treatment protocol on results of a series of studies performed previously [17, 21, 26, 27], in which different concentrations of elastase were used to degrade elastin fibers in different tissues. These studies were performed experiments in the presence or absence of soybean trypsin inhibitor (SBTI). We used pancreatic elastase (E1250, Sigma, St. Louis, MO), as a potent elastin degrading enzyme, in combination with SBTI (T9003, Sigma, St. Louis, MO) to minimize non-specific enzymatic activity of elastase [12, 42]. Preliminary tests revealed that 16 h of treatment in a physiological solution under gentle agitation at 37 °C with a volume activity of 3 U/mL elastase and 0.1 mg/mL SBTI was sufficient for the purpose of this study. The left disc of each head was assigned to the control (PBS) group (n=5) and the right disc to the treated (elastase) group (n=5). All discs were mechanically tested before and after incubation with PBS or elastase, thus serving as their own controls. After the pre-treatment mechanical test, samples were relaxed in PBS for 30 min at room temperature. Then samples were distributed to vials containing PBS or elastase solution and incubated accordingly. Following treatment, the samples were washed in three changes of PBS for 5 min each under gentile agitation at room temperature before undergoing the post-treatment mechanical test with the protocol described in the “Mechanical loading experiment” section.

2. 3. Immunofluorescence

To visualize the effect of elastase treatment, 3 pairs of TMJ discs were used for immunohistochemistry and included in the PBS

or elastase treatment without undergoing any mechanical test. Porcine arteries were used as positive controls for elastin staining. Following treatment, samples were washed with PBS, fixed overnight in 4% paraformaldehyde and subsequently placed in PBS at 4 °C until cryosectioning. For that purpose, the central, lateral and medial parts of the disc were cut into two parts, one used for transverse and the other for sagittal sectioning. Then, each part was placed on a specimen holder using Tissue-Tek (Sakura Finetek, Netherlands), and sectioned at 10 µm. The artery specimens were sectioned transversely.

The sections were incubated with PBS followed by blocking buffer (1% BSA, 20% goat serum, PBS) for 20 min. The sections were then incubated with a cocktail of primary antibodies containing rabbit polyclonal anti-collagen I (1:1000, ab34710; Abcam, MA) and mouse polyclonal anti-elastin (1:100, ab9519; Abcam) overnight at 4 °C. Thereafter, sections were washed with PBS and a cocktail of secondary antibodies containing Alexa 488 goat anti-rabbit (1:2000; Invitrogen, CA) and Alexa 647 goat anti-mouse (1:200; Invitrogen, CA) was added for 1 h. Then, sections were washed with PBS, stained with 4’,6-diamidino-2-phenylindole (DAPI) for 10 min, washed in PBS mounted with Vectashield mounting medium (Vector laboratories, CA) and stored at 4 °C. Images were obtained with an inverted confocal microscope (Leica SP8, Leica, Germany) using a ×40 oil immersion objective with zoom factor of ×1 and pinhole adjusted to 5 airy units. Recordings were further processed with ImageJ (NIH, MD).

2.4. Transmission electron microscopy (TEM)

Cartilage samples were fixed at ambient temperature in 4% paraformaldehyde and 1% glutardialdehyde in 0.1 M Sodium cacodylate buffer for 24 h. The samples were subsequently washed in buffer and postfixed in 1% OsO4 for 1 h. Then, the tissue was dehydrated in a series of ethanol, and embedded in epoxy resin (LX-112). Ultrathin sections were made from the tissue blocks using a diamond knife. Sections were stained with uranyl acetate and lead nitrate and examined in a CM10 Philips electron microscope.

2. 5. Collagen tortuosity analysis

Collagen tortuosity index, as a measure of collagen fiber waviness, was calculated from the microscopy images based on the Gabor wavelet algorithm previously developed in MATLAB (Mathwork, MA) [43]. In short, Gabor wavelets with a range of different wavelengths (2, 3, 4, 5) and orientations $(0, \pi/4, \pi/2, \pi)$ were convolved with the images, and corresponding histograms were obtained. The tortuosity index was then calculated by deducting the maximum number in the Gabor histograms from 1. Thus, the tortuosity index values varied between 0 and 1. If the tortuosity index is 0, the fibers are completely straight, and if tortuosity index is 1, the tortuosity of fibers is maximal.

2. 6. Cell shape analysis

Using DAPI images, cell shape index was quantified in MATLAB (Mathwork, MA) as previously described [44]. In brief, a binary threshold was applied to the gradient images after the images were converted to a grey-scale format and the noises were

reduced. After removal of small artefacts by a geometrical filter, Shape Index (SI) as a measure of cell elongation was calculated as $SI = (4\pi \times area) / perimeter^2$. If a cell is fully circular, it has a shape index of 1, and if it is a line, it has a shape index of zero.

2. 7. Tissue volume quantification

To assess the effect of elastase treatment on the general morphological aspects of the disc, we measured the volume of the samples before and after PBS/elastase treatment. For that purpose, a measuring cylinder was filled with 20 mL of PBS. Before treatment, the disc was gently placed inside the cylinder causing an increase of PBS level, which was marked and imaged accordingly. The same process was repeated after treatment. Then, we measured the difference between the marked points on the cylinder using Image (NIH, MD) allowing us to calculate the volume changes of the disc following the PBS/elastase treatment.

2. 8. Biochemical analysis

Following the post-treatment mechanical test, the samples were relaxed in PBS for 30 min at room temperature. To determine the extent of degradation, we excised two adjacent specimens from each of the five mechanically tested regions using a 4-mm disposable dermal punch (Miltex Instruments, Lake Success, NY). The specimens were placed in vials, frozen in liquid nitrogen, sealed and stored at -80 °C until testing. From each pair of adjacent specimens, one was assigned to hydroxyproline and GAG content measurement and the other was used for elastin quantification. The total hydroxyproline and GAG content were determined according to Ghazanfari et al. [43]. Accordingly, the assigned specimen was lyophilized overnight, dry weighted and digested by papain (Sigma, St. Louis, MO) for 16 h. GAG content was quantified by 1-9-dimethylmethylene blue dye-binding assay using chondroitin sulfate from shark cartilage (Sigma, St. Louis, MO) to create a standard curve. The hydroxyproline, as a measure of total collagen content, was determined by alkaline autoclaving of the papain digest followed by spectrophotometric quantification of its reaction with chloramine-T and dimethylaminobenzaldehyde. The elastin content was quantified following the Fastin elastin colorimetric assay protocol (Biocolor Ltd., UK). As previously described [45], samples were wet weighted and then digested by oxalic acid, solubilizing insoluble elastin into-elastin polypeptides, which later were quantified along with soluble tropoelastin spectrophotometrically.

2. 9. Experimental apparatus

To characterize the mechanical properties of the samples, we used a custom-built materials testing machine [46] with a resolution of 1 μm at a rate of maximally 30 Hz. It consists of two 4 mm circular flat-ended indenters (stainless-steel) and a chamber. One indenter is fixed at the center inside the chamber and aligned with the upper indenter, which applies cyclic compressive displacement controlled by a custom-made software (implemented in LabVIEW 8.2, National Instruments, Austin, TX). A 25 N load cell (Honeywell Model 11, Honeywell, Golden Valley, MN) was used to register the normal reaction force applied to the top indenter. The load cell was connected to a bridge amplifier (HBM K10, HBM, Darmstadt, Germany). After A/D conversion (NI USB 6008, National Instruments, Austin, TX), the signals were registered by the same software controlling the displacing indenter.

With this setup, displacement and reaction force were recorded simultaneously at a 16 ms interval.

2. 10. Mechanical loading experiment

We determined the regional mechanical properties of the samples using the protocol developed previously [47]. Frozen discs were immersed in PBS and thawed at room temperature for 1 h. Then, using cyanoacrylate (Histoacryl, Braun Surgical S.A., Rubi, Spain), the inferior surface of the desired region was glued to the bottom indenter and the chamber was filled with PBS allowing the disc to equilibrate for 5 min. Next, a tare load of 0.02 N was applied to the sample to prevent slippage and provide a full contact between the indenter, and the disc. Following another 5 min of relaxation time, the platen-to-platen distance was measured by a digital caliper and defined as the thickness of the sample. To obtain a reproducible loading pattern, samples were preconditioned for 3 min through a series of cyclic compressive displacements corresponding to 10% strain at a frequency of 1 Hz. Following 5 min recovery time, samples were loaded for another 20 cycles similar to the preconditioning loading protocol. When done, the disc was carefully detached from the bottom indenter, glued at another region and mechanically tested using the same protocol. The loading protocol was chosen based on the physiological loading during human mastication. Reportedly, the joint space reduces up to 10% during maximum clenching [48]. Regarding the chewing frequency, although porcine masticates faster than a human (2-3 Hz) [49], previous studies using a porcine model [50, 51] reported their mechanical data at 1 Hz, which is shown to be the mean frequency of human mastication (0.5-1.5 Hz) [49].

Stress (force divided by cross-sectional area of the indenter) and strain (upper indenter displacement divided by the specimen thickness) were driven from load-displacement data using routines written in Matlab (MathWorks, Inc., Natick, MA). For evalution of the mechanical data, we focused on the following terms: 1) instantaneous modulus defined as the ratio of maximum stress occurring at the first cycle to its corresponding strain and; 2) maximum hysteresis calculated from the enclosed area of the first loop of stress-strain curve, called maximum energy dissipation.

2. 11. Statistical analysis

Initially, to rule out any significant biological variation in the pre-treatment (before PBS/elastase treatment) mechanical properties, we performed a paired Student's t-test between the corresponding single regions of the left and right samples. We also used the same analysis to determine any significant difference between the left and right disc volume before the PBS/elastase treatment. Given no significant pre-treatment differences between either mechanical properties or the disc volume of both sides, we carried out further analysis by only having the post-treatment (after PBS/elastase treatment) mechanical data and disc volume measurements taken into account. We applied a two-way analysis of variance (ANOVA) with repeated measurements to compare two overall factors of elastase treatment and disc region on the mechanical and biochemical measurements of the associated groups. A multiple pairwise comparison with Bonferroni's correction was performed to investigate the regional differences within each group. The adjusted p-values were used for comparisons. Additionally, a paired Student's t-test determined the differences between the corresponding

single regions of the control (PBS) and treated (elastase) groups. To analyze the differences of collagen tortuosity and cell shape indices between the control (PBS) and treated (elastase) groups, we calculated the average of indices in separate regions and then compared the mean of all regions indices between the two groups using an unpaired Student's t-test. Furthermore, a paired Student's t-test was used to compare the differences between the average of disc volumes in the control (PBS) and elastase treated groups.

Statistical analyses were performed using GraphPad Prism 6.01 (GraphPad Software, La Jolla, CA) using a significance level of $p<0.05$.

3. Results

3.1. Immunofluorescence

The immunofluorescence staining of the control (PBS) samples revealed fairly straight, long and branching elastin fibers interlacing heterogeneously through the densely packed and highly organized collagenous network across the disc (Figs. 1 and 2). More specifically, collagen fibers were seen anteroposteriorly oriented in the intermediate regions, merging to the encircling fibers at the periphery and forming a fibrillar network (Figs. 1 and S. 3). The elastin fibers were occasionally branching at acute angles and reuniting into straight or oblique fibers with a preferential alignment mainly parallel to collagen fibers (Figs. 1 and S. 2). In the AB where the collagen fibers seemed more isotropic, the elastin fibers appeared more oblique with higher branching frequency forming random patterns (Figs. 1 and S. 2). Sagittal sections further demonstrated the presence of elastin fibers throughout the full thickness of the disc (Figs. 2, S.1 and S. 5) with straight elastin fibers in the IZC running along the collagen fibers and extending to the AB and PB where they display more branching and random patterns of distribution. The immunofluorescence staining of the treated (elastase) samples clearly showed loss of elastin compared to the control (PBS) group (Fig. 2). Notably, as the degradation begins at the exterior surfaces, the effectiveness of elastase varied throughout the thickness, leaving behind different degrees of digestion. The effect of degradation was most pronounced in the thinnest zone of the disc, intermediate region (IZC, IZM, IZL), leading to extensive fragmentation, diminishing of elastin fibers and sporadic remnants of elastin fragments (Figs. 1, 2, S. 2 and S. 5). In the bands (AB and PB) of the disc however, due to their higher thickness, the elastase incubation resulted in less fragmentation but enough to create regions containing loose, sparse and coiled elastin fibers (Figs. 1, 2, S. 2 and S. 5). The orientation of collagen fibers seemed unaffected by elastase degradation (Figs. 1, 2, S. 3 and S. 6). Following elastase treatment, we observed severe degradation of elastin fibers, disorganization of collagen fibers and disappearance of cell nuclei in the media and intima layers of porcine artery compared to the control (PBS) sample (Fig. S. 8).

3.2. Tissue volume

The disc volume before and after PBS/elastase treatment was quantified. We found a significant increase of disc volume in the treated (elastase) group (Fig. 3A).

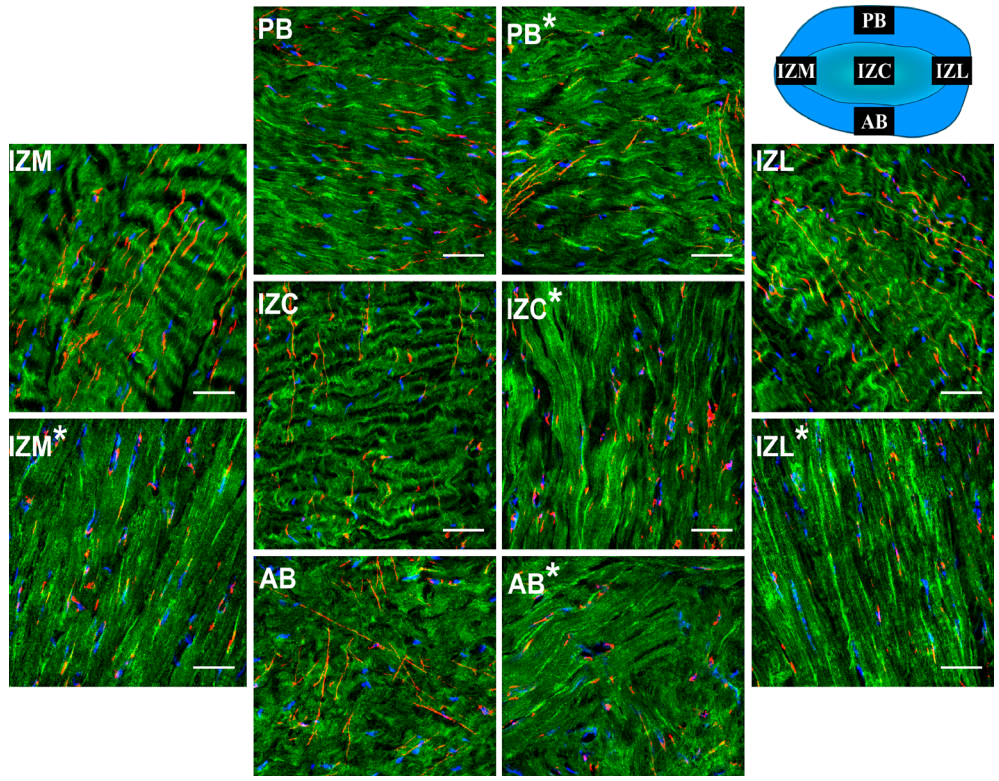

Fig. 1. Top view confocal image and overlay immunofluorescence staining of elastin fibers, collagen fibers type I and cell nuclei of porcine TMJ disc before and after elastase treatment. Elastin fibers, collagen fibers type I and cell nuclei can be distinguished in red, green and blue, respectively. The schematic configuration of the TMJ disc (seen from top), placed in the uppermost right corner of the figure exhibits the location of different regions of the TMJ disc and the direction of imaging (top view). Region labels with asterisk present the treated (elastase) samples. Anteroposteriorly aligned collagen fibers in the intermediate regions (IZC, IZM and IZL) merge with fibers at the peripheral bands (PB and AB), forming a dense collagenous network. Note the frequent oblique elastin fibers criss-crossing through the isotropic collagenous network at the AB, while in other regions elastin fibers are mainly aligned parallel with collagen fibers. Following the elastase treatment (regions with asterisk) the elastin fibers are fragmented, patched and diminished across the TMJ disc. Also, note the reduction of collagen fibers tortuosity and cell nuclei elongation following the elastase treatment (regions with asterisk), with more noticeable impact in the intermediate regions (IZC, IZM and IZL). Scale bar: 50 μm. For more clarity, refer to Fig. S. 2, Fig. S. 3 and Fig. S. 4, presenting immunofluorescence staining of elastin fibers, collagen fibers type I and cell nuclei in separate channels, respectively.

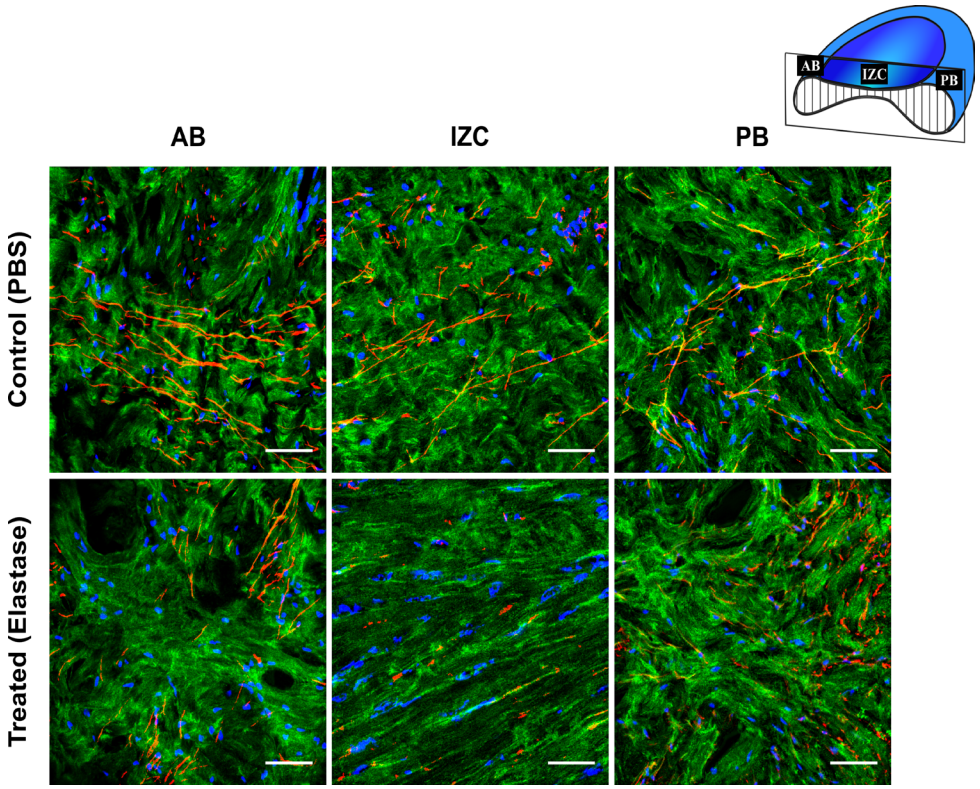

Fig. 2. Sagittal view confocal image and immunofluorescence staining of elastin fibers, collagen fibers type I and cell nuclei of porcine TMJ disc before and after elastase treatment. Elastin fibers, collagen fibers type I and cell nuclei can be distinguished in red, green and blue, respectively. The schematic configuration of the TMJ disc sagittal cross-section, placed in the uppermost right corner of the figure exhibits the location of different regions of the TMJ disc. The upper row shows images of different regions in the control (PBS) samples and the lower row shows the treated (elastase) ones. The collagen fibers, running anteroposteriorly in the IZC, extend to the AB and PB where they merged with fibers mainly aligned mediolaterally (perpendicular to the plane). The elastin fibers, running parallel to the collagen fibers in the IZC, also extend to the AB and PB where they show less directivity. Following the elastase treatment, the elastin fibers are fragmented, patched and diminished across the TMJ disc sagittal cross-section. Also, note the reduction of collagen fibers tortuosity and cell nuclei elongation following the elastase treatment with more noticeable impact in the intermediate regions (IZC, IZM and IZL). Scale bar: 50 μm. For more clarity, refer to supplemental Figs. S. 5, S. 6 and S. 7, presenting immunofluorescence staining of elastin fibers, collagen fibers type I and cell nuclei in separate channels, respectively.

3. 3. Collagen tortuosity

Comparing indices between the two groups showed that the degree of fiber tortuosity in the treated (elastase) samples was significantly smaller than the control (PBS) samples (Fig. 3B). As the fibers' tortuosity decreased from left to right, their corresponding indices decreased accordingly (Fig. 3C).

3. 4. Cell shape

The results presented in Fig. 3D show that cells were significantly elongated following elastase treatment. The shape index changed from 1 to 0 as the shape geometry shifted from line to circle (Fig. 3E).

3. 5. Biochemical analysis

3. 5. 1. Elastin

The elastin content for the control (PBS) and treated (elastase) groups are presented in Fig. 4A. Elastase treatment reduced the average elastin content of the disc by 40%. Two-way ANOVA showed an overall significant effect of elastase treatment ($p<0.0001$) and disc region ($p<0.0001$) on the elastin content across the TMJ disc. More specifically, elastase treatment significantly reduced elastin content across the thinnest regions as in IZC (52%), IZM (47%,) and IZL (49%) while the thicker regions, AB and PB were less affected. Additionally, multiple pairwise post-hoc test found regional differences of elastin content in the control (PBS) group with IZC possessing the highest amount of elastin, which was in turn significantly different from IZM, IZL and AB. In the treated (elastase) samples, however, regional variation of the elastin content seemed to have a different pattern with PB containing the highest remnant of elastin, which was significantly different from IZC, IZM, IZL and AB.

3. 5. 2. Collagen

The collagen content of the control (PBS) and treated (elastase) groups are presented in Fig. 4B. Following the elastase treatment, the average collagen content of the disc was reduced by 22%. The two-way ANOVA revealed an overall significant effect of elastase treatment ($p<0.0001$) and disc region ($p<0.05$) on collagen content across the TMJ disc. Additionally, analysis of the collagen content between the control and treated groups within a single region showed significant reduction of the collagen content across the thinnest regions as in IZC (13%), IZM (16%) and IZL (32%), while the thicker regions, AB and PB, had a limited reduction.

3. 5. 3. GAG

Fig. 4C. shows the GAG content of the control (PBS) and treated (elastase) samples. Following elastase treatment, there was an average of 41% reduction in GAG content of the disc. Two-way ANOVA revealed an overall significant effect of elastase treatment ($p<0.001$) and disc region ($p<0.05$) on the GAG content across the TMJ disc. Specifically, the effect of elastase treatment was significantly pronounced in the IZC (55%), IZM (51%), IZL (40%), and AB (35%), while in the PB, the elastin was reduced to a small extent. Furthermore, multiple pairwise post-hoc test expressed regional variation of the GAG content in the control (PBS) group as PB possesses significantly lower amount of GAG compared to IZC, IZM and IZL. The regional heterogeneity of GAG content was lost following the elastase treatment.

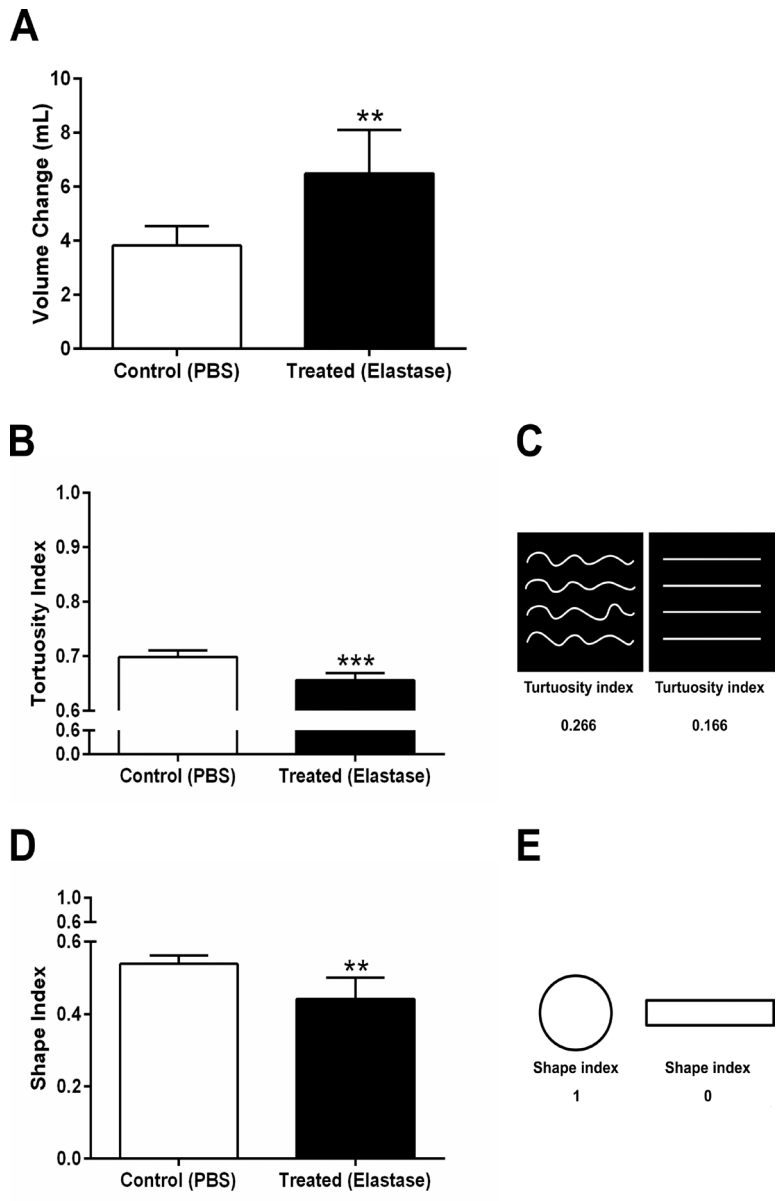

Fig. 3. Effect of elastase treatment on volume, cell shape and collagen fibers tortuosity of the porcine TMJ disc. (A) TMJ disc volume. (B) Average of quantified tortuosity indices obtained from all regions of the TMJ disc. (C) Average of quantified cell shape indices obtained from all regions of the TMJ disc. All data are presented as mean ± SD. ** indicates $p<0.01$, and *** indicates $p<0.001$.

3. 6. Mechanical properties

Fig. 5. shows the representative mechanical behavior of the IZC in the TMJ disc, before and after elastase treatment. The stress-strain curve (Fig. 5A) showed a nonlinear behavior and a Mullins effect also after the elastase treatment. The average of maximal energy dissipation across the disc was increased by approximately 40% following the elastase treatment and the stress-strain curve continuously shifted down while that of the control (PBS) disc relaxed after a few consecutive cycles (Fig. 5A). The continuous downward shifting of the stress-strain curve is partially reflected in the corresponding stress-time graph (Fig. 5B) as the stress peaks did not level off like the control (PBS) disc.

The two-way ANOVA revealed a significant effect of elastase treatment ($p<0.001$) and disc region ($p<0.0001$) on the maximal energy dissipation of the disc. The intermediate regions were affected most as the maximal energy dissipation of the disc was significantly increased in IZC (91%), IZM (57%) and IZL (139%), while the thicker regions, AB and PB, merely experienced minor changes (Fig. 6A). Furthermore, multiple pairwise post-hoc test showed regional variations in the control group as the PB had a significantly higher maximal energy dissipation compared to the IZL. Following elastase treatment, maximal energy dissipation appeared to be the least in the AB, which was significantly different with IZC and IZM.

The effect of elastase treatment on the compressive instantaneous modulus of the disc is illustrated in Fig. 6B. Two-way ANOVA only revealed a significant effect of the disc region ($p<0.0001$) on the maximal energy dissipation. Following elastase treatment, there seemed to be a noticeable upward trend of instantaneous modulus in the thinnest regions (IZC, IZM and IZL). In contrast, the thicker regions showed a decreasing response to the treatment, which was significantly pronounced in the AB (46%) and not significant in the PB. Additionally, multiple pairwise post-hoc test showed that the instantaneous modulus was regionally different in the control group as both AB and PB were significantly stiffer than IZC and IZL. The treaded (elastase) group did not show any regional differences of instantaneous modulus.

3. 7. TEM

A representative image of the IZC region of the control (PBS) disc (Fig. 7) demonstrates a densely-packed and highly-ordered array of collagen fibrils with their characteristic D-periodic banding pattern. With regard to the elastin fibers, we observed microfibrils both independently and in close association with amorphous elastin core, forming mature elastin fibers (Fig. 7A). Notably, these fibers were intimately associated to and ran parallel to the collagen fibrils (Fig. 7A). Following elastase digestion, we could not identify any type of elastin fiber except some elastin devoid areas appeared in collagen interfibrillar spaces, containing some delicate microfibrils and seemingly remnants of elastin. These interfibrillar void spaces may be a potential indication of partially digested elastin fibers (Fig. 7B). Furthermore, the collagen fibrils seemed to be less densely-packed; nonetheless the orientation of the fibrils was retained (Fig. 7B).

4. Discussion

The purpose of this study was to provide a systematic structural-functional

characterization of elastin fibers in the TMJ disc. Using a top-down approach by selectively degrading elastin fibers, in combinatio nwith assessment of mechanical, structural and compositional changes in the native and degenerated discs, equipped us with a powerful analytical arsenal to better understand the nature and the extent of the elastin fiber contribution to the TMJ disc biomechanics.

Our study indicates a crucial and complex structural-functional role of elastin fibers in the disc. Immunofluorescent localization of elastin revealed that elastase treatment of the disc resulted in a varying extent of elastin fragmentation especially in the intermediate zone (IZC, IZM and IZL; Figs. 1 and S. 2) where most changes occurred. Interestingly, as byproducts of perturbing the elastin fibers network, we found a significant volume enlargement of the disc (Fig. 3A), reduction of collagen fibers tortuosity (Fig. 3B) and cell shape elongation (Fig. 3D).

Biochemical analysis confirmed the efficacy of the elastase treatment and its corresponding structural changes by showing significant reduction of elastin (Fig. 4A), collagen (Fig. 4B) and GAG (Fig. 4C) content in the reported regions. The resultant effect of these structural and compositional changes was evidently reflected in the altered viscoelastic mechanical properties of the disc (Figs. 5 and 6).

Following elastase treatment, the Mullins effect and nonlinear stiffening behavior of the control (PBS) group (Fig. 5A) still occurred in the corresponding stress-strain curves, meaning that the progressive engagement of collagen fibers were still taking place. Despite the degradation and reduction of elastin in different regions, the treated (elastase) discs appeared to be elastic enough to retreat back to the zero-strain state during the unloading cycle (Fig. 5A). However, the treated (elastase) samples were experiencing continuous softening likely associated with inability of tissue to recover completely (remnant strains). This observation is in accordance with Schriefl et al. [26] as they also observed continuous softening in elastase treated samples attributed to the continuous elongation of the tissue over the loading cycles.

In agreement with Yu et al. [52], we observed elastin fibers forming cross-bridge connectivity between adjacent collagen fibers, especially in the AB (Figs. 1, 2, S. 2 and S. 5). Probably, the collagen fibers are no longer anchored to the matrix or to one another at locations emptied from the elastin fibers (Fig. 7), and hence they are able to separate, rearrange and slide against each other more easily. The regions with significant loss of elastin fibers (IZC, IZM and IZL; Fig. 4A) exhibited significant increase of maximal energy dissipation (Fig. 6A). Given the higher thickness in the AB and PB, our confocal images showed only partial degradation of elastin fibers (Figs. 1, 2, S. 2 and S. 5) in these regions, leaving more elastin fibers through the collagenous network; consequently, limited changes of their hysteresis properties (Fig. 6A) were observed.

Elastase treatment of the disc also resulted in regionally different values of the instantaneous modulus (Fig. 6B). However, unlike the hysteresis data, two-way ANOVA did not reveal an overall significant effect of elastase treatment on the instantaneous modulus. This may be due to the fact that its calculation is based on the maximal point (higher strain range) of the stress-strain loading curve where the mechanical

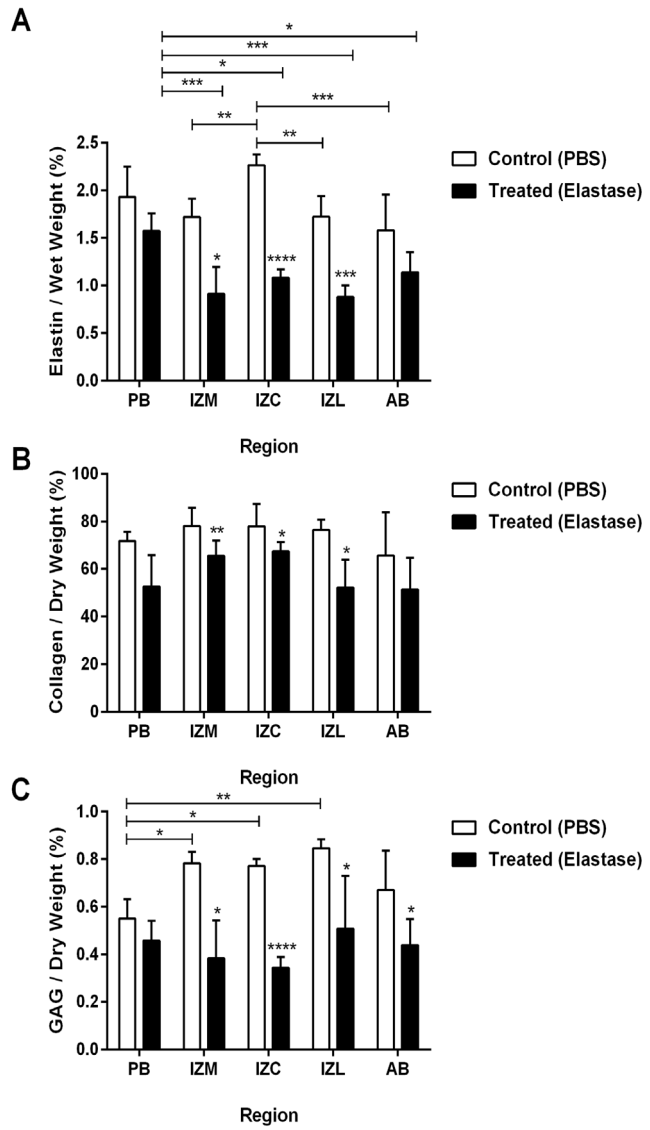

Fig. 4. Effect of elastase treatment on elastin (A), collagen (B) and GAG (C) content of the porcine TMJ disc. After elastase treatment, the elastin content was significantly reduced in the intermediate regions (IZC, IZM and IZL) and the heterogeneous distribution of elastin content was changed. Elastase treatment resulted in a significant reduction of collagen content in the intermediate regions (IZC, IZM and IZL). The elastase treatment significantly reduced the GAG content in the intermediate regions (IZC, IZM and IZL) and AB. All data are presented as mean ± SD. * indicates $p<0.05$, ** indicates $p<0.01$, *** indicates $p<0.001$ and **** indicates $p<0.0001$.

behavior of the tissue is primarily governed by collagen fiber [25]. In accordance with previous studies [17, 20, 26, 53], we observed an increasing trend of the modulus in the intermediate zone of the treated (elastase) discs, especially in the IZC and IZL. This stiffer behavior can be explained by a significant reduction of the collagen fibers tortuosity across the treated (elastase) discs, with more noticeable effect in the intermediate zone (Fig. 6B), yielding to collagen recruitment at lower strains. This phenomenon highlights a vital mechanical function of elastin fibers in the TMJ disc as they could provide shock absorption, taking up small strains and thereby shielding collagen fibers against repetitive impact loading. This mechanism has also been suggested in experiments with elastase treatment of other tissues [17, 20, 22, 26, 53]. Elastase treatment also caused a significant enlargement of disc volume (Fig. 3A), in line with other forms of size enlargement reported previously [20, 26, 54]. In fact, this could explain the interconnection between the elastin fibers and collagen crimp, as the origin of the latter has been associated with a pre-stress induced by elastin fibers along the collagen fibers axis during dehydration of the matrix [55, 56]. With elastin being removed, the existing pre-stress on collagen fibers is abolished, leaving them in a relaxed state. Another study [57] suggested a cell-induced mechanism involving traction forces generated by fibrocartilage cells, which buckles the collagen fibers and create a periodic crimp structure. However, this view is opposed by Ghazanfari et al. [43] who found formation of collagen crimps upon the appearance of elastin fibers in tissue engineered constructs. In light of this perspective, considering the collagen fibers acting as a contact guidance for the cells, having them straightened following the elastase digestion forces the cells elongate accordingly [58]. The significant elongation of cells (Figs. S. 4 and S. 7) after elastase treatment in our study might support this theory, but we cannot confirm it without further experiments.

The reduction of instantaneous modulus in the AB and PB is likely due to differences in orientation of collagen and elastin fibers, biochemical composition and thickness, which all impede the diffusion of elastase and compromise its degradative role. This is in line with a study of Chow et al. [20] in which the elastase was used to degrade elastin fibers in porcine aortas with five different incubation periods and reported four different stages of mechanical behavior (see Fig. 6 therein). This has been attributed to the different structure of elastin lamella and uneven degradation of elastin fibers due to the thickness. In fact, Shi et al. [59] reported an isotropic diffusivity of fluid in the AB of native porcine TMJ disc, due to its multi-directional fibrillar arrangement, emphasizing the potential mechanical consequence of perturbing this fibrillar organization on the load-bearing capacity of the AB.

Interestingly, we found that elastase treatment caused significant reduction of collagen fibers and GAG content in some regions of the disc (Fig. 4B and 4C). It has been shown that elastase is selective but not specific [60], being capable of degrading a broad range of substrates in the ECM. Indeed, elastase has been described as a powerful agent, facilitating collagen degradation by de-masking collagen fibers through removal of the ground substance such as GAG and elastin, as well as depolymerizing the insoluble collagen [60] or even directly denaturing the collagen fibers as reported previously [42]. By contrast, although collagenase is considered as the

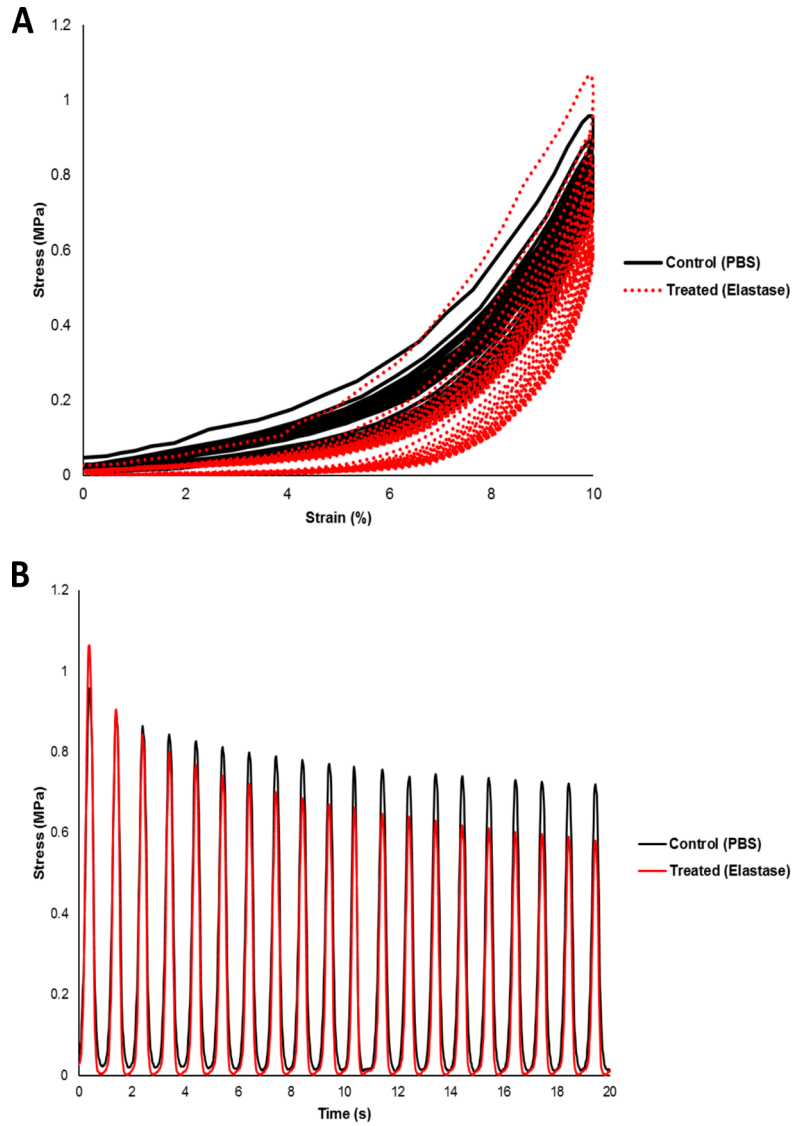

Fig. 5. Effect of elastase treatment on the stress response of the intermediate regions (IZC, IZM and IZL) in the porcine TMJ disc during cyclic loading. The control (PBS) data (black) and treated (elastase) data (red) indicate the mechanical changes induced by elastase treatment in (A) mechanical hysteresis graph and (B) stress-time graph. Note the increase of maximal energy dissipation (A) and the continuous softening behavior of the treated (elastase) disc (A and B).

main collagenolytic enzyme, it cannot digest the highly crosslinked insoluble collagen polymers [12]. This may explain the limited reduction of collagen content after the collagenase digestion of the TMJ disc in our previous study [47] *vis-à-vis* the corresponding results we obtained after elastase digestion in this study. Despite the presence of SBTI in our enzymatic solution, reduction of collagen content was not completely prevented. This finding is in agreement with other studies who also reported different extent of this non-specific degradation in presence [27] or absence [20, 21] of SBTI. Despite this inevitable side effect of elastase, we conclude that the mechanical changes in our study should not be attributed solely to the contribution of remaining collagenous network but to the fragmentation and reduction of elastin fibers. This is of significant importance as we observed a completely different structural and mechanical response to the collagenase digestion in our previous study [47]. We found a strong reduction of the instantaneous modulus and maximal energy dissipation in all regions of the collagenase treated disc (manifested in a highly linear stress-strain curve; see Fig. 4 therein), despite a minimal reduction of collagen content in the corresponding regions. We attributed this intriguing effect to a severe structural disorganization of collagenous network caused by collagenase digestion (see Fig. 7 and 8 therein). In the present study, however, the elastase treatment did not affect the structural alignment of collagen fibrils (Fig. 7), which was manifested in the still occurring nonlinearity and the Mullins effect in their stress-strain curve (Fig. 5A).

Contextualizing the inferred properties within complex kinematics of the TMJ disc provides us a better insight into the functional role of elastin fibers. It has been suggested that the superior layer of the bilaminar zone (posterior attachment) of the disc acts as an antagonist, limiting the anterior-medial displacement of the disc while storing the produced strain energy during the jaw opening [61, 62]. During the closing movement, the highly resilient superior layer of the bilaminar zone couples with the posterior distal traction of non-elastic inferior one, thereby restoring the disc back to its resting posture through an interaction with the masticatory muscles [61, 62]. According to Scapino [63] however, the bilaminar zone is considered as a hydraulic device in which elastin fibers facilitate fast fluid redistribution in the cavities to promote the congruent movement of the TMJ disc. Compared to the hyaline cartilage, given the low amount of GAG content in the disc suggests that elastin fibers compensate their associated restorative role by recoiling the collagen fibers and the disc back to the pre-stressed state, thereby maintaining the homeostatic form of the disc upon load removal during the jaw movement [4, 64]. Our data supports this mechanism by showing the reduction of collagen tortuosity and volume enlargement of the disc after the elastase treatment.

In light of the presented findings, any structural and compositional changes of elastin fibers caused naturally through aging or pathologically as in degenerative conditions is of clinical importance. The elastin content is reported to decrease through advancing age and is not only accountable for the loss of elasticity of tissues but also provokes structural changes of collagenous network, potentially leading to irreversible mechanical changes in the tissue [53]. Elastolysis could also occur in case of an imbalance between the activated degradative proteases and the functional inhibitory- initiate or exacerbate a self-reinforcing

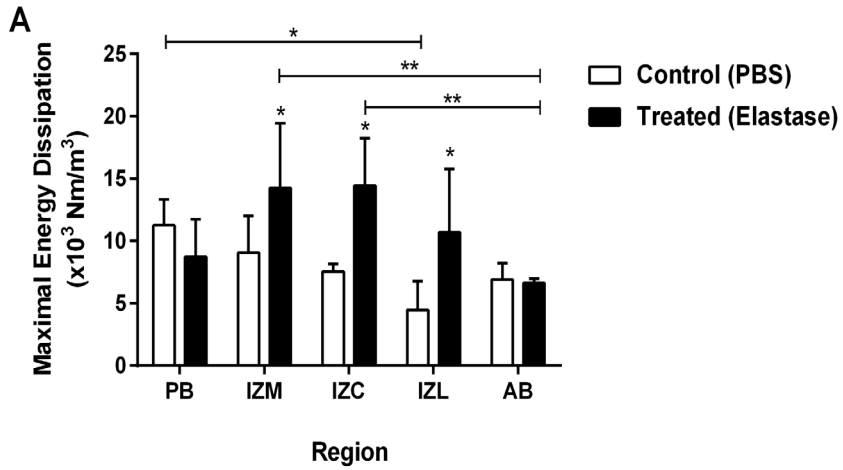

Fig. 6. Effect of elastase treatment on mechanical compressive properties of the porcine TMJ disc. (A) Following elastase treatment, the maximal energy dissipation was significantly increased in the intermediate regions (IZC, IZM and IZL) while decreased minimally in the AB and PB. The regional variation in the control (PBS) samples was only observed between PB and IZL, with the former being significantly higher. However, this pattern was changed after elastase treatment with IZC an IZM being higher than AB. (B) The effect of elastase treatment on the instantaneous modulus of the disc found to be pronounced only in the AB where the stiffness reduced significantly. Also, there seemed to be a general increasing trend in the instantaneous modulus of the intermediate regions. All data are presented as mean ± SD.
* indicates $p<0.05$, and ** indicates $p<0.01$

degenerative process, referred as the "vicious circle" by Vergroesen et al. [65] (see Fig. 2 therein). Fragmentation of elastin fibers and depletion of elastin are considered to be common characteristics of aneurysms [20]. Regarding the diarthrodial joint, a higher level of elastase has been reported in the synovial fluid of rheumatoid arthritis [66, 67]. As in case of the TMJ, different components are exposed to the synovial fluid, which could be affected by presence of proteases in it. For example, reduction of elastin fibers has been observed in the bilaminar zone of TMJ discs with anterior displacement [68]. We show here that degradation of elastin fibers influences its viscoelastic properties; this could subject it to unfavorable biomechanics during the jaw movement; thereby affecting kinematics of the TMJ disc. This may lead to malpositioning of the disc relative to the mandibular and condylar bone, known as internal derangement [69].

Overall, the elastin fibers, despite their low quantity in the TMJ disc ECM, revealed some remarkable structural-functional properties, vital to the TMJ disc biomechanics. The elastase treatment resulted in region-dependent mechanical, structural and compositional changes in the TMJ disc. Degradation of elastin fibers resulted in volume expansion of the TMJ disc, reduction of collagen tortuosity and cell elongation, indicating a release of a pre-stress responsible for holding up the homeostatic configuration of the disc. Given the intimate connection of elastin fibers with collagenous network, having them degraded resulted in a less confined rearrangement and incomplete recoil of collagen fibers during cyclic loading. These results point out the contribution of elastin fibers to the TMJ disc biomechanics goes beyond merely a recovering role; influencing on the viscoelastic properties of the disc through an interaction, mainly with collagen fibers and other ECM components. It is hoped that this study offers a better insight on the potential degradative contribution of elastase in pathophysiological conditions and also provides a stepping stone toward development of new and improved tissue engineering strategies by bringing elastin fibers into the perspective.

4.1. Limitations

In this study, we chose the porcine TMJ disc material as it has been identified similar to the human model regarding its morphology, biochemical composition and function [70]. Also, we used this model, so that we can compare our results with our previous study [47], in which we investigated the mechanical, biochemical and structural effects of collagenase treatment using a similar experimental setup. We did not intend to use the "equivalent" concentration of collagenase for our elastase solution, as that could not be meaningfully determined. Also, we did not aim for complete degradation and depletion of the elastin fibers as the samples had to be integrated enough following the treatment, so we could perform the post-treatment mechanical loading test. Given the differential degradation of elastin fibers, and unavoidable reduction of collagen fibers caused by nonspecific elastase activity, distinguishing the individual mechanical contribution of elastin fibers is challenging. Schriefl et al. [26] used human abdominal aortas and tried to find out the optimal concentration of SBTI to combine with elastase solution to avoid the non-specific effect of degradation on the collagen fibers. They tried varying amounts of SBTI and found that adding amounts above 600 μg/mL PBS can negatively affect the elastolysis. While they reported that half

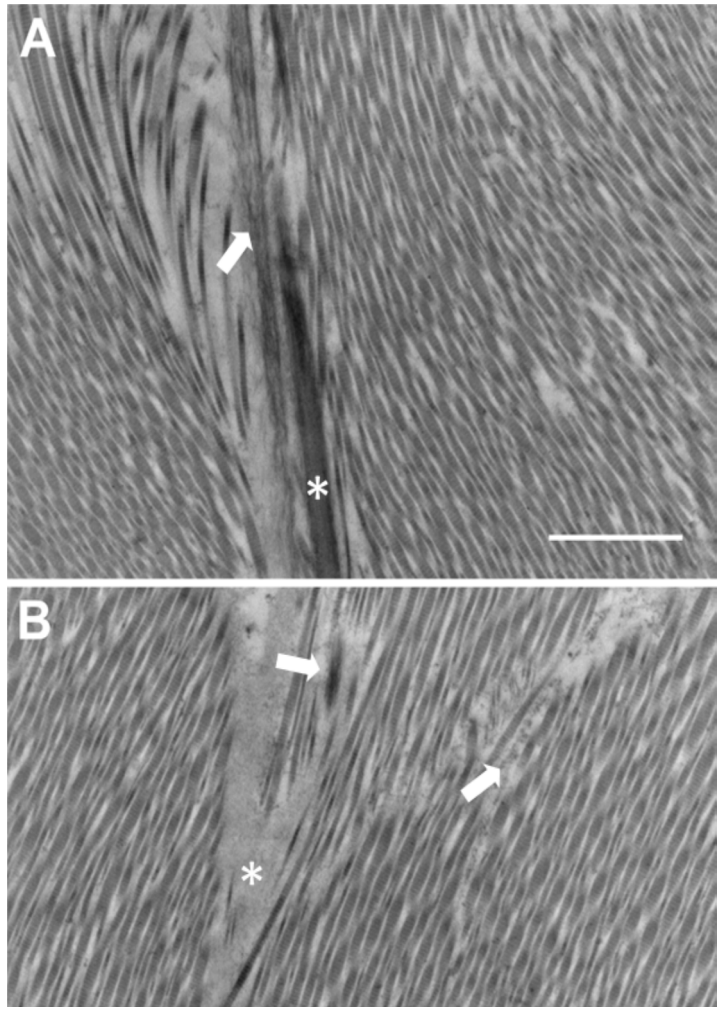

Fig. 7. Transmission electron micrographs of IZC of porcine TMJ disc before (A) and after (B) elastase treatment. (A) Two different stages of elastin fiber development are visible: 1) the premature elastin fiber (white arrowhead) is seen as microfibrils, assembling together to create a layout where elastin will be deposited. Also, a mature elastin fiber (white asterisk) can be recognized by its amorphous elastin core and surrounding microfibrils. These fibers seem to be running along the collagen fibrils, which are distinguishable by their distinctive D-periodic banding pattern. (B) Following elastase treatment, we could hardly spot any elastin fibers, except some elastin devoid areas in the middle of collagen fibrils (white asterisk), seemingly containing some remnants of microfibrils (white arrowhead) and elastin. Except the appearance of these void spaces, the collagen fibrils arrangement did not seem to be affected following the elastase treatment. Scale bar: 2 μm.

of above-mentioned concentration provided partial degradation of elastin fibers, which served the purpose of their study based on their type of tissue, elastase concentration and treatment time, it still could only prevent “some” collagen digestion. Therefore, the nonspecific activity of elastase remains to be an open issue.

It is important to note that we could not find any relevant study in the literate of the TMJ disc which involves any forms of mechanical assessment of elastase treated samples. Therefore, we discussed our data with regard to other studies that performed experiments, similar in nature, but using different tissues and mechanical loading protocol. The most important difference to consider is that unlike ours, all of these studies investigated the role of elastin under tensile loading while we used compression as it is one of the common types of load applied on the TMJ disc [71]. More importantly, we wanted to have a meaningful comparison with our previous study [47] where we used the same mechanical loading regimen to study mechanical properties of the collagenase treated samples.

5. Acknowledgment

The authors would like to thank Sara Ghazanfari for her great help in data analyses.

References

1. Tanaka E, and Koolstra JH. Biomechanics of the temporomandibular joint. J Dent Res. 2008 Nov;87(11):989-991.

2. Tanaka E, and van Eijden T. Biomechanical behavior of the temporomandibular joint disc. Crit Rev Oral Biol Med. Crit Rev Oral Biol Med. 2003;14(2):138-150.

3. Detamore MS, and Athanasiou KA. Structure and function of the temporomandibular joint disc: implications for tissue engineering. J Oral Maxillofac Surg. 2003 Apr;61(4):494-506.

4. Detamore MS, et al. Quantitative analysis and comparative regional investigation of the extracellular matrix of the porcine temporomandibular joint disc. Matrix Biol. 2005 Feb;24(1):45-57.

5. Almarza AJ, et al. Biochemical analysis of the porcine temporomandibular joint disc. Br J Oral Maxillofac Surg. 2006 Apr;44(2):124-128.

6. Tanaka E, et al. Dynamic shear properties of the temporomandibular joint disc. J Dent Res. 2003 Mar;82(3):228-231.

7. Detamore MS, and Athanasiou KA. Tensile properties of the porcine temporomandibular joint disc. J Biomech Eng. 2003 Aug;125(4):558-565.

8. Schiffman E, et al. Diagnostic Criteria for Temporomandibular Disorders (DC/TMD) for Clinical and Research Applications: recommendations of the International RDC/TMD Consortium Network* and Orofacial Pain Special Interest Group†. J Oral Facial Pain Headache. 2014 Winter;28(1):6-27.

9. Farrar WB, and McCarty WL. The TMJ dilemma. J Ala Dent Assoc. 1979 Winter;63(1):19-26.

10. Tanaka E, Detamore MS, and Mercuri LG. Degenerative disorders of the temporomandibular joint: etiology, diagnosis, and treatment. J Dent Res. 2008 Apr;87(4):296-307.

11. de Bont LG, and Stegenga B. Pathology of temporomandibular joint internal derangement and osteoarthrosis. Int J Oral Maxillofac Surg. 1993 Apr;22(2):71-74.

12. Sedowofia KA, et al. Collagenolytic enzyme systems in human intervertebral disc: their control, mechanism, and their possible role in the initiation of biomechanical failure. Spine (Phila Pa 1976). 1982 May-Jun;7(3):213-222.

13. Visse R, and Nagase H. Matrix metalloproteinases and tissue inhibitors of metalloproteinases. Circ Res. 2003 May 2;92(8):827-839.

14. Planello AC, et al. Association of matrix metalloproteinase gene polymorphism with temporomandibular joint degeneration. Eur J Oral Sci. 2011 Feb;119(1):1-6.

15. Klein T, and Bischoff R. Physiology and pathophysiology of matrix metalloproteases. Amino Acids. 2011 Jul;41(2):271-290.

16. Henninger HB, et al. Effect of elastin digestion on the quasi-static tensile response of medial collateral ligament. J Orthop Res. 2013 Aug;31(8):1226-1233.

17. Lee TC, et al. The effect of elastin damage on the mechanics of the aortic valve. J Biomech. 2001 Feb;34(2):203-210.

18. Weisbecker H, et al. The role of elastin and collagen in the softening behavior of the human thoracic aortic media. J Biomech. 2013 Jul 26;46(11):1859-1865.

19. Lee AY, et al. Effects of elastin degradation and surrounding matrix support on artery stability. Am J Physiol Heart Circ Physiol. 2012 Feb 15;302(4):H873-884.

20. Chow MJ, et al. Progressive structural and biomechanical changes in elastin degraded aorta. Biomech Model Mechanobiol. 2013 Apr;12(2):361-372.

21. Barbir A, et al. Effects of enzymatic digestion on compressive properties of rat intervertebral discs. J Biomech. 2010 Apr 19;43(6):1067-1073.

22. Yapp C, and Chen Q. The Mechanical, Structural, and Compositional Changes of Tendon Exposed to Elastase. Ann Biomed Eng. Ann Biomed Eng. 2015 Oct;43(10):2477-2486.

23. Thambyah A, and Broom N. Micro-anatomical response of cartilage-on-bone to compression: mechanisms of deformation within and beyond the directly loaded matrix. J Anat. 2006 Nov;209(5):611-622.

24. Broom ND, and Marra DL. New Structural Concepts of Articular Cartilage Demonstrated with A Physical Model. Connect Tissue Res. 1985;14(1):1-8.

25. Roach MR, and Burton AC. The reason for the shape of the distensibility curves of arteries. Can J Biochem Physiol. 1957 Aug;35(8):681-690.

26. Schriefl AJ, et al. Selective enzymatic removal of elastin and collagen from human abdominal aortas: uniaxial mechanical response and constitutive modeling. Acta Biomater. 2015 Apr;17:125-136.

27. Smith LJ, et al. Elastic fibers enhance the mechanical integrity of the human lumbar anulus fibrosus in the radial direction. Ann Biomed Eng. 2008 Feb;36(2):214-223.

28. Reihsner R, et al. Biomechanical properties of elastase treated palmar aponeuroses. Connect Tissue Res. 1991;26(1-2):77-86.

29. Mills DK, Fiandaca DJ, and Scapino RP. Morphologic, microscopic, and immunohistochemical investigations into the function of the primate TMJ disc. J Orofac Pain. 1994 Spring;8(2):136-154.

30. O'Dell NL, et al. Morphological and biochemical studies of the elastic fibres in the craniomandibular joint articular disc of the tight-skin mouse. Arch Oral Biol. 1996 May;41(5):431-437.

31. Mah J. Histochemistry of the foetal human temporomandibular joint articular disc. Eur J Orthod. 2004 Aug;26(4):359-365.

32. Griffin C, and Sharpe C. Distribution of elastic tissue in the human temporomandibular meniscus especially in respect to "compression" areas. Aust Dent J. 1962;7:72-78.

33. Savalle WP, et al. Elastic and collagenous fibers in the temporomandibular joint capsule of the rabbit and their functional relevance. Anat Rec. 1990 Jun;227(2):159-166.

34. Frommer J, and Monroe C. Development and distribution of elastic fibers in the mandibular joint of the mouse. A comparison of fetal, suckling, juvenile and adult stages. Anat Rec. 1966 Jan;156: 333-345.

35. Iwai-Liao Y, et al. Scanning electron microscopy of elastic system fibers in the articular disc of the rat mandibular joint. Okajimas Folia Anat Jpn. 1994 Oct;71(4):211-225.

36. O'Dell NL, Sharawy M, and Starcher BC. In vitro effects of elastase on rabbit craniomandibular joint articular disks. Cells Tissues Organs. 1992;145(3):229.

37. Clément C, et al. Quantitative analysis of the elastic fibres in the human temporomandibular articular disc and its attachments. Int J Oral Maxillofac Surg. 2006 Dec;35(12):1120-1126.

38. Gross A, Bumann A, and Hoffmeister B. Elastic fibers in the human temporo-mandibular joint disc. Int J Oral Maxillofac Surg. 1999 Dec;28(6):464-468.

39. Keith DA. Elastin in the bovine mandibular joint. Arch Oral Biol. 1979;24(3):211-215.

40. O'Dell NL, et al. Morphological and biochemical evidence for elastic fibres in the syrian hamster temporomandibular joint disc. Arch Oral Biol. 1990;35(10):807-811.

41. Scapino RP, Obrez A, and Greising D. Organization and Function of the Collagen Fiber System in the Human Temporomandibular Joint Disk and Its Attachments. Cells Tissues Organs. 2006;182(3-4):201-225.

42. Kafienah W, et al. Cleavage of native type I collagen by human neutrophil elastase. Biochem J. 1998 Mar 1;330 (Pt 2):897-902.

43. Ghazanfari S, et al. In Vivo Collagen Remodeling in the Vascular Wall of Decellularized Stented Tissue-Engineered Heart Valves. Tissue Eng Part A. 2015 Aug;21(15-16):2206-2215.

44. Ghazanfari S, and Tafazzoli M. Analysis of alterations in morphologic characteristics of mesenchymal stem cells by mechanical stimulation during differentiation into smooth muscle cells. Cell J. 2010;12(1): 73-80

45. Ghazanfari S, et al. Collagen Matrix Remodeling In Stented Pulmonary-arteries After Trans-apical Heart Valve Replacement. Cells Tissues Organs. 2016;201(3):159-169.

46. Berendsen AD, et al. Three-Dimensional Loading Model for Periodontal Ligament Regeneration In Vitro. Tissue Eng Part C Methods. 2009 Dec;15(4):561-570.

47. Fazaeli S, et al. The contribution of collagen fibers to the mechanical compressive properties of the temporomandibular joint disc. Osteoarthritis Cartilage. 2016 Jul;24(7):1292-1301.

48. Kuboki T, et al. Effect of occlusal appliances and clenching on the internally deranged TMJ space. J Orofac Pain. 1999 Winter;13(1):38-48.

49. Druzinsky RE. The Time Allometry of Mammalian Chewing Movements: Chewing Frequency Scales with Body Mass in Mammals. J Theor Biol. 1993 Feb 21;160(4):427-440.

50. Lumpkins SB, and McFetridge PS. Regional variations in the viscoelastic compressive properties of the temporomandibular joint disc and implications toward tissue engineering. J Biomed Mater Res A. 2009 Sep 1;90(3):784-791.

51. Tanaka E, et al. Dynamic compressive properties of porcine temporomandibular joint disc. Eur J Oral Sci. 2003 Oct;111(5):434-439.

52. Yu J, et al. Microfibrils, elastin fibres and collagen fibres in the human intervertebral disc and bovine tail disc. J Anat. 2007;210(4):460.

53. Fonck E, et al. Effect of elastin degradation on carotid wall mechanics as assessed by a constituent-based biomechanical model. Am J Physiol Heart Circ Physiol. 2007 Jun;292(6):H2754-2763.

54. Dobrin PB, Baker WH, and Gley WC. Elastolytic and collagenolytic studies of arteries. Implications for the mechanical properties of aneurysms. Arch Surg. 1984 Apr;119(4):405-409.

55. Vesely I. The role of elastin in aortic valve mechanics. J Biomech. 1998 Feb;31(2):115-123.

56. Nakagawa H, Mikawa Y, and Watanabe R. Elastin in the Human Posterior Longitudinal Ligament and Spinal Dura A Histologic and Biochemical Study. Spine (Phila Pa 1976). 1994 Oct 1;19(19):2164-2169.

57. Shah JS, Palacios E, and Palacios L. Development of crimp morphology and cellular changes in chick tendons. Dev Biol. 1982 Dec;94(2): 499-504.

58. Ghazanfari S, Khademhosseini A, and Smit TH. Mechanisms of lamellar collagen formation in connective tissues. Biomaterials. 2016 Aug;97:74-84.

59. Shi C, et al. Relationship between anisotropic diffusion properties and tissue morphology in porcine TMJ disc. Osteoarthritis Cartilage. 2013 Apr;21(4):625-633.

60. Ujiie Y, et al. Degradation of noncollagenous components by neutrophil elastase reduces the mechanical strength of rat periodontal ligament. J Periodontal Res. 2008 Feb;43(1):22-31.

61. Takisawa A, Ihara K, and Jinguji Y. Fibro-architectonics of human temporomandibular joint. Okajimas Folia Anat Jpn. 1982 Aug;59(2-3):141-166.

62. Osborn JW. The disc of the human temporomandibular joint: design, function and failure. J Oral Rehabil. 1985 Jul;12(4):279-293.

63. Scapino RP. The posterior attachment: its structure, function, and appearance in TMJ imaging studies. Part 1. J Craniomandib Disord. 1991 Spring;5(2):83-95.

64. Mills DK, Daniel JC, and Scapino R. Histological features and in-vitro proteoglycan synthesis in the rabbit craniomandibular joint disc. Arch Oral Biol. 1988;33(3):195-202.

65. Vergroesen PP, et al. Mechanics and biology in intervertebral disc degeneration: a vicious circle. Osteoarthritis Cartilage. 2015;23(7):1057-1070.

66. Virca GD, et al. Quantitation of Human Leukocyte Elastase, Cathepsin G, α-2-Macro-Globulin and α-1-Proteinase Inhibitor in Osteoarthrosis and Rheumatoid Arthritis Synovial Fluids. Adv Exp Med Biol. 1984;167:345-353.

67. Huet G, et al. Measurement of elastase and cysteine proteinases in synovial fluid of patients with rheumatoid arthritis, sero-negative spondylarthropathies, and osteoarthritis. Clin Chem. 1992 Sep;38(9):1694-1697.

68. Hall MB, Brown RW, and Baughman RA. Histologic appearance of the bilaminar zone in internal derangement of the temporomandibular joint. Oral Surg Oral Med Oral Pathol. 1984 Oct;58(4):375-381.

69. Senga K, et al. Ultrastructural study on adhesions in internal derangement of the temporomandibular joint. J Oral Maxillofac Surg. 1999 Feb;57(2):165-170.

70. Kalpakci KN, et al. An Interspecies Comparison of the Temporomandibular Joint Disc. J Dent Res. 2011 Feb;90(2):193-198.

71. Beek M, et al. Dynamic Properties of the Human Temporomandibular Joint Disc. J Dent Res. 2001 Mar;80(3):876-880.